



Universiteit
Leiden
The Netherlands

Generating High B_0 -Fields for use in Extremely Low Temperature MRFM

Plugge, Jaimy

Citation

Plugge, J. (2020). *Generating High B_0 -Fields for use in Extremely Low Temperature MRFM*.

Version: Not Applicable (or Unknown)

License: [License to inclusion and publication of a Bachelor or Master thesis in the Leiden University Student Repository](#)

Downloaded from: <https://hdl.handle.net/1887/94289>

Note: To cite this publication please use the final published version (if applicable).



Generating High B_0 -fields for use in Extremely Low Temperature MRFM

THESIS

submitted in partial fulfillment of the
requirements for the degree of

MASTER OF SCIENCE

in

PHYSICS

Author : Jaimy Plugge
Student ID : s1654845
Supervisor : Prof. Dr. Ir. Tjerk H. Oosterkamp
Tim M. Fuchs MSc
 2^{nd} corrector : Prof. Dr. Jan M. Van Ruitenbeek

Leiden, The Netherlands, March 11, 2020

Generating High B_0 -fields for use in Extremely Low Temperature MRFM

Jaimy Plugge

Huygens-Kamerlingh Onnes Laboratory, Leiden University
P.O. Box 9500, 2300 RA Leiden, The Netherlands

March 11, 2020

Abstract

In this thesis, we address our progress to send high currents and generating high magnetic fields at milliKelvin temperatures for the use in MRFM measurements. Multiple ways for sending a current while at $20mK$ inside a dilution refrigerator are described. The use of a heatsink and an option for splitting the current over multifilament connections are analyzed and tested. We find starting resistances in our spotwelds contradicting with earlier measurements of $3p\Omega$ conducted in our group.

Next, the design of a transformer in the form of a cone complement is showed and preliminary tests are presented. Furthermore, the inductance is calculated from a sweep over a frequency range from $500Hz$ to $20kHz$.

Our measurements show high potential for an experiment to generate $500mT$ at $20mK$. This experiment is described and in addition, a possible use for B_1 -fields of this cone complement coil is briefly discussed.

Contents

| | | |
|----------|-------------------------------------|-----------|
| 1 | Introduction | 1 |
| 1.1 | Nuclear Magnetic Resonance | 1 |
| 1.2 | Magnetic Resonance Force Microscopy | 2 |
| 1.3 | Persistent Current Switch | 3 |
| 1.4 | In this thesis | 3 |
| 2 | Theory | 5 |
| 2.1 | Dilution Refrigerator | 5 |
| 2.2 | High Currents | 7 |
| 2.3 | Heat Sink | 7 |
| 2.4 | Persistent Current Switch | 8 |
| 2.4.1 | Transformer | 8 |
| 2.4.2 | Coil Inductance | 8 |
| 3 | Methodology | 11 |
| 3.1 | High Currents | 11 |
| 3.2 | Persistent Current Switch | 13 |
| 4 | Results | 15 |
| 4.1 | High Currents | 15 |
| 4.2 | Persistent Current Switch | 18 |
| 5 | Discussion | 21 |
| 5.1 | High Currents | 21 |
| 5.2 | Persistent Current Switch | 22 |
| 5.3 | B_1 possibilities | 23 |
| 6 | Conclusion | 25 |
| 6.1 | Acknowledgments | 25 |
| | Bibliography | 27 |

1

Introduction

Most microscopy techniques are only able to image the surface of a sample or up to a specific (low) penetration depth, since they depend on photons or electrons interacting with the sample. For a lot of physical properties, it is interesting to image the bulk or the 3D structure of the sample. One example in the biology is being able to image whole protein structures or DNA to better understand their working. Besides, such technique could also be used to better understand superconductivity. Furthermore, if we are then able to get a system interacting with only a single electron, the limits of quantum mechanics can be explored[1]. Evidently, then, a microscopy technique capable of imaging the bulk of a sample must be constructed.

1.1 Nuclear Magnetic Resonance

Nuclear Magnetic Resonance (NMR) is a widely used method to differentiate between different chemical substances with the most known application being MRI-scanners in hospitals. The core of NMR includes a static magnetic field (B_0) which polarizes the spins in a sample and an RF-pulse (B_1) perpendicular to B_0 to manipulate those spins. Classically, this can be explained as a B_1 -field producing a torque which causes the spins to rotate, the amount of rotation depends on the duration and the magnetic field strength of the pulse. After the spins have rotated to the desired tip angle, the RF-pulse is turned off. Since the B_0 -field is always present, the spins want to realign to that field which takes a relaxation time T_1 . This T_1 is substance dependent and this dependence is used to differentiate between different (chemical) substances[2].

1.2 Magnetic Resonance Force Microscopy

To obtain a better spatial resolution, magnetic resonance force microscopy (MRFM) was proposed by J.A. Sidles[3]. MRFM replaces the pickupcoil used in standard NMR techniques to obtain the signal by a mechanical resonator, of which the motion is coupled through magnetic dipole interactions to the sample. In most MRFM setups, the sample is placed on the cantilever which is then positioned above a magnet which provides the B_0 field. In the Oosterkamp Group however, a small magnet ($\sim \mu m$, see figure 1.1) is attached to the tip of the cantilever and positioned above the sample. This magnet functions as both the source B_0 -field and acts as somewhat of an antenna coupled to the pickupcoil. This pickupcoil is connected to a Superconducting Quantum Interference Device (SQUID) which is capable of sensing extremely small changes in the magnetic field. This setup makes it possible to sense an even smaller number of spins than the more common MRFM method discussed before. Since we want

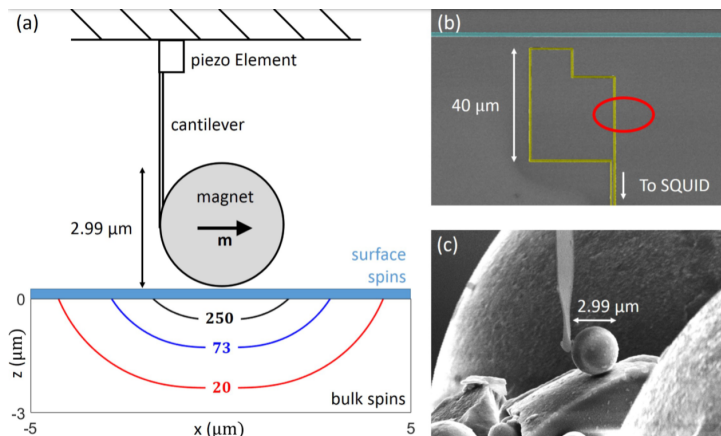


Figure 1.1: [4] a) Schematic overview of the MRFM setup used in the Oosterkamp Group. In b), the pickuploop can be seen and c) is an STM image of the tip of the cantilever.

to measure small fluctuations of the cantilever motion, we want to reduce noise fluctuations as much as possible. This can partly be achieved by placing the whole experiment inside a dilution refrigerator capable of cooling to $10mK$. At this temperature, thermal fluctuations play a much smaller role than at room temperature and the whole experiment is vibration isolated to decrease the influence of outside vibrations.

1.3 Persistent Current Switch

Since we want as little noise in our magnetic field as possible, a Persistent Current Switch (PCS) capable of operating at millikelvin temperatures[5] must be used. A PCS switches between the normal and superconducting state of a wire that shortcuts a coil in our experiment. In the normal state of the shortcut wire, the system acts as an RL-circuit and in the superconducting state of the shortcut wire, a current can flow without resistance. A scheme of the circuit can be seen in figure 1.2.

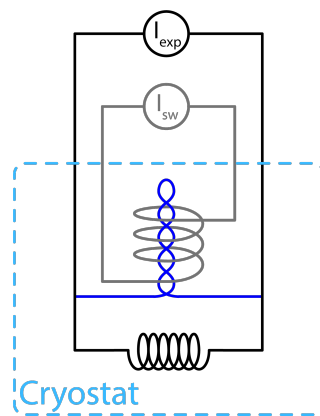


Figure 1.2: The circuit scheme of a PCS.

To switch between these two states, the superconducting wire is placed inside a coil. If a high enough magnetic field is generated by that coil, it will break the superconducting state of the wire. If we then turn off the magnetic field, the superconducting state of the wire will be restored and a current is able to flow from the coil through the shortcut wire and back into the coil without noise coming from the resistance or from disturbances coming from outside the cryostat. To construct this, we need to use a shortcut wire with a low enough critical field for us to be able to achieve this state change. In addition, we need to be able to generate that magnetic field. Since magnetic field scales linearly with the current through the coil, we have to be able to send a high current through the coil.

1.4 In this thesis

This thesis will describe the experiments and discuss the results of our ideas for sending high currents and creating large magnetic fields. In the

next chapter, *Theory*, the rough principal of a dilution refrigerator is discussed. Furthermore, we will go over the challenges involved in sending high currents at low temperatures and provide a possible solution in the form of a heatsink. We end this chapter with transformers and induction of our coil in the Persistent Current Switch. In chapter 3, *Methodolgy*, we describe our experiments of which the results can be found in chapter 4. These results are discussed in chapter 5 and a follow up experiment based on the results is introduced. A conclusion of our research can then be found in chapter 6.

2

Theory

This chapter will describe the theory that is needed to understand the experiments described in this thesis. The theory behind the dilution refrigerator is kept very brief, for further explanation, we refer the reader to [6].

2.1 Dilution Refrigerator

As already explained in section 1.2, it is important for our experiments to be at mK temperatures. This can be achieved by the use of a dilution refrigerator. Heinz London first proposed the dilution refrigerator in 1951 and first experimental realization was achieved by P. Das et al.[7] in 1965. Two types of dilution refrigerators exist, a wet dilution refrigerator and a dry dilution refrigerator with the difference of them being the way in which they precool their ${}^3\text{He}$. Inside the dry dilution refrigerator, the system is first cooled down to $\sim 3K$ by compressing and decompressing *Helium* (He) with for example a pulse tube. From that point, further cooling is achieved by mixing the isotopes ${}^3\text{He}$ with ${}^4\text{He}$. The ${}^3\text{He}$ is pumped down into the *mixing chamber*. In this mixing chamber, two separate phases of ${}^3\text{He}$ are in equilibrium, a concentrated phase of pure ${}^3\text{He}$ gas and a dilute phase in which ${}^3\text{He}$ is mixed with liquid ${}^4\text{He}$. Inside the mixture, there is a tube with a conical still at the end, here the ${}^3\text{He}$ vaporizes and is then being pumped into the system again. The pressure and temperature inside the still are kept at the correct values to only vaporize ${}^3\text{He}$. This causes the ${}^3\text{He}$ inside the bath of ${}^4\text{He}$ to diffuse into the pipe to the still. This results in a deficit of ${}^3\text{He}$ inside the mixture. To re-equilibrate, the ${}^3\text{He}$ from the concentrated phase will go through the phase boundary which is an endothermic process. This cools down the mixing chamber and with this method, temperatures of $2mK$ can be achieved[8]. Most experiments in this thesis are done in the *Marshmallow*, one of the dilution refrigerators

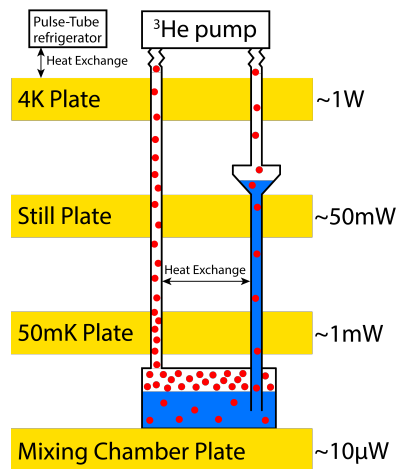


Figure 2.1: A sketch of our dilution refrigerator, ${}^3\text{He}$ is depicted by the red dots and the ${}^4\text{He}$ is blue. Next to the arrows in the figure which show the heat exchange, there is also heat exchange between the plates and the pipes going through them.

used by the Oosterkamp Group, with the other being the *Yeti* and *Olaf*. Unless stated otherwise, the experiments were done in the *Marshmallow*.

2.2 High Currents

In section 1.3, we explained why we need to be able to send high currents. The problem with this, is that we cannot simply send higher currents, as we want to minimize the thermal load while sending these currents. Since the power in a wire is given by

$$P = I^2R, \quad (2.1)$$

a higher current (I) results in more heat dissipation. This can be resolved by the use of superconducting cables, since zero resistance (R) implies zero heat dissipation. So as long as our wires remain superconducting, our dissipation will equal zero. Superconducting materials are defined by a few properties, which yield defined quantities. Of these, we will discuss the critical temperature T_c and the critical field H_c . These critical values define the upper boundary of our experiments, if either $T > T_c$ or $H > H_c$, the superconducting state will be broken and the material will start conducting resistively. We will use *NbTi* for our experiments, a widely used superconductor for electromagnets thanks to its relatively high critical temperature of 10K and critical field of 15T[9].

The problem we face is that the connectors are still resistive and will thus dissipate heat to our cable. This heating can break the superconducting state in our wire which will result in even more heat dissipation. This is the main challenge we want to solve.

2.3 Heat Sink

While superconductors are excellent at conducting electrical signals, they are very bad heat conductors. So any incoming heatflux will not easily be dissipated. Practically, this means that a cable heating because of its connector will lose its superconducting state rapidly. To counteract this, the wire can be run in contact with a good heat conductor. Then, the additional heat does not have to flow through the superconductor anymore, but can be dissipated through the heat conductor into one of the plates of the dilution refrigerator. A device made for this purpose is called a heatsink.

2.4 Persistent Current Switch

As already explained in section 1.3, a persistent current switch consists of a wire that switches from the superconducting state to the normal state and back due to an applied magnetic field. To obtain a high enough magnetic field (100mT for tantalum) without having to send high currents (< 400mA) through resistive cables, a superconducting transformer is used.

2.4.1 Transformer

The ratio of current on the secondary and the primary side of a transformer is given by

$$\frac{I_S}{I_P} = k \cdot \frac{N_P}{N_S} \quad , \quad (2.2)$$

with N_P and N_S the amount of windings on the primary and secondary side respectively. The inductive coupling between the two coils of the transformer is given by k which we expect to be equal to ~ 0.8 . Instead of this k , we can also use an effective amount of primary windings $\tilde{N}_P = k \cdot N_P = 72$. For easier calculation and to give a lower bound, we say $\tilde{N}_P \equiv 70$.

2.4.2 Coil Inductance

To get a better understanding of the coil, it is important to calculate the inductance. The inductance can be calculated via the energy inside the coil (figure 2.2) of which the design is further explained in section 3.2. For

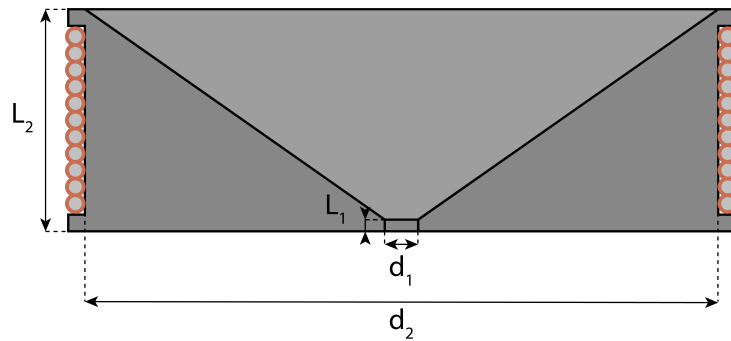


Figure 2.2: Schematic image of the coil and the transformer. Dimensions are: $L_1 = 0.699mm$, $L_2 = 5.25mm$, $d_1 = 1mm$ and $d_2 = 14mm$.

this, we first have to calculate the magnetic field inside the coil which is

given by

$$B = \mu_0 n I = \mu_0 \frac{\tilde{N}_P}{L_2} I \quad (2.3)$$

We expect the magnetic field to be $\frac{L_2}{L_1}$ higher at the end of the "funnel" of the cone complement. The magnetic field there, when calculated using the formula for an infinitely long solenoid, is

$$B = \mu_0 \frac{\tilde{N}_P}{L_1} I \quad (2.4)$$

The energy stored in the coil must be the same as the energy stored in the magnetic field, so

$$\frac{1}{2} L I^2 = \frac{1}{2 \mu_0} B^2 V \quad (2.5)$$

Solving for L and using the expression for the magnetic field of equation 2.4 yields:

$$\begin{aligned} L &= \frac{1}{\mu_0} \left(\frac{B}{I} \right)^2 V \\ &= \frac{1}{\mu_0} \left(\frac{B}{I} \right)^2 \cdot L_1 \pi \left(\frac{d_1}{2} \right)^2 \\ &= \frac{\mu_0 \tilde{N}_P^2}{L_1} \cdot \pi \left(\frac{d_1}{2} \right)^2 \end{aligned} \quad (2.6)$$

We expect this calculated inductance to deviate from the actual value since it is a very short solenoid. This is why we also measured the inductance. The impedance of an inductor can be calculated from

$$Z_L = \frac{U_L}{i \omega I_L} = \frac{U_L}{2 \pi f I_L} \quad , \quad (2.7)$$

here U_L is the voltage over the coil and I_L is the current through the coil. Since the i only describes a phase shift of 90° , we will ignore it for the calculation of the inductance. The circuit in figure 2.3 describes how one could perform this measurement. We know the resistances to each be $\sim 12 \Omega$ and since series resistance can be added up, for the full circuit of the current we can just set the total resistance to be 24Ω . So if we then apply an oscillating voltage V_{osc} with a known frequency across the circuit, I_L can be replaced by $\frac{V_{osc}}{R}$ and formula 2.7 can be worked out. From this, the inductance can be calculated since in our case, $Z_L = L$.

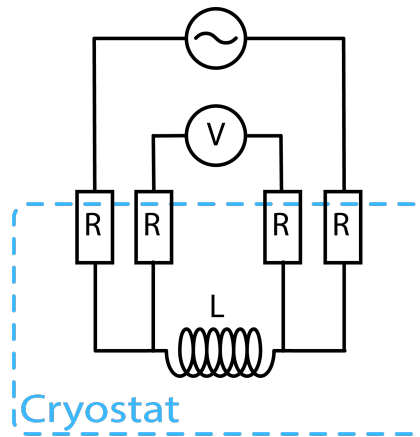


Figure 2.3: The circuit used to measure the inductance. The fraction of the resistive cables out of the cryostat with respect to the resistive cables inside the cryostat is not in proportion.

3

Methodology

In this chapter, we will go over our heatsink concepts. Furthermore, an idea to split the current over multiple cables is discussed. Last, the design and principal of our Cone Complement coil is explained.

3.1 High Currents

As explained in section 2.2, we want to address the heating caused by the dissipation in the connectors. One proposed method to counteract this problem, is to make use of a heatsink. Single filament *NbTi* in copper wires (Supercon T48B-M $62\mu\text{m}$ filament diameter) are run along a piece of copper which is connected to one of the plates of our dilution refrigerator. With this setup, the heat will be able to flow through the copper instead of the wire since the copper is a better heatconductor.

The first plan for the heatsink is to spotweld our *NbTi* wires to $100\mu\text{m}$ thick Niobiumfoil and glue the niobiumfoil with GE-varnish to a piece of copper. To make sure that there is no electrical contact between the copper and the Niobiumfoil, rolling paper for cigarettes is placed between them since it is a very thin insulator. GE-varnish is used because of it's relatively high heat conductance at low temperatures. The schematic overview of this spotwelded heatsink is shown in figure 3.1.

Instead of spotwelding the wire onto a piece of Niobiumfoil, it can also be soldered onto copper sheets with superconducting solder. These copper sheets are then glued onto a copper plate with GE-varnish and a rolling paper between them. The advantage of this method is that the wires are directly connected to copper which improves the heat conductance, the disadvantage is that we do not have a single continuous superconductor through which the current has to flow. For this method $350\mu\text{m}$ copper sheets are completely covered with *Pb60Sn40* solder ($T_C > 4\text{K}$) and then the stripped *NbTi* wires are placed into the solder as close to the copper as

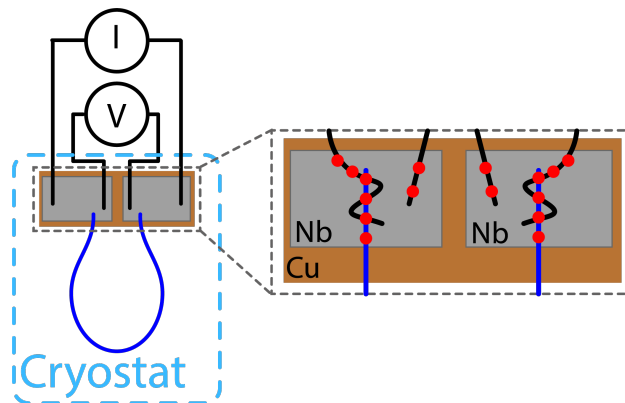


Figure 3.1: The schematic overview of the spotwelded heatsink, the spotwelds are depicted by the red dots.

possible to obtain the best heat conductance. To make sure the current has to flow close to the copper sheets to improve heat conductance, the layer of solder is made very thin between the two soldered wires.

Rather than finding a way for the heat to flow away from the connectors, the heat dissipation itself can also be addressed. This is done by dividing the current over multiple connectors to lower the overall resistance and thus lowering the dissipated power in these elements. The setup is shown in figure 3.2.

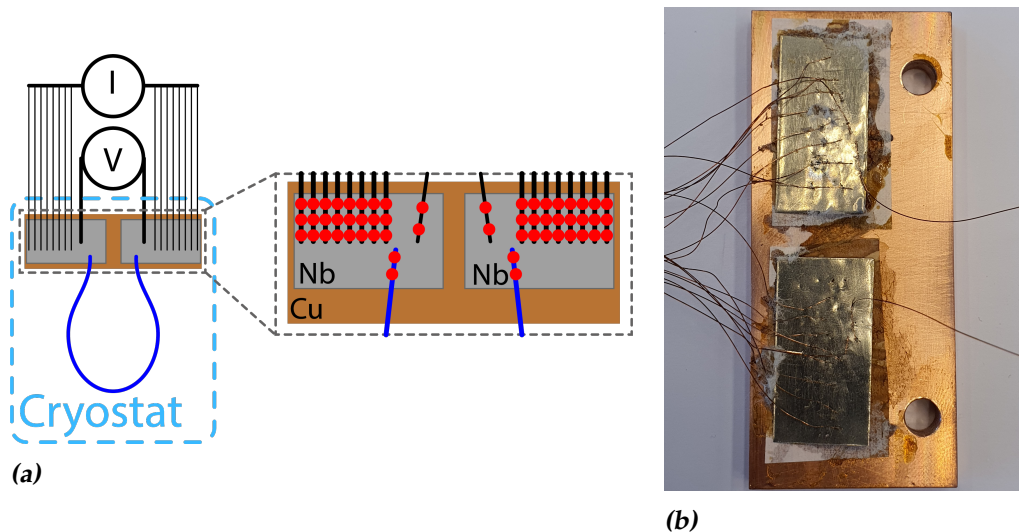


Figure 3.2: a) A schematic overview of the current splitter, the spotwelds are depicted by the red dots. b) A photo of the current splitter.

Since the voltage is the same for all elements of a parallel circuit, the

current for this circuit is given by

$$I_{total} = V \left(\sum_{i=1}^8 \frac{1}{R_i} \right) \quad (3.1)$$

But since we expect the resistance of each cable to be equal, we obtain:

$$I_{total} = V \left(\frac{8}{R} \right) = 8 \cdot \frac{V}{R} = 8 \cdot I_{individual} \quad (3.2)$$

This equation shows that the current gets evenly divided over the 8 cables and since $P = I^2 R$, the power per resistive element of the circuit becomes 64 times smaller. Since we have 8 of these paths, we get to a total dissipated power 8 times smaller than we would expect from a single path.

3.2 Persistent Current Switch

A proposed method for generating high magnetic fields is to design a cone complement from a *Niobium* rod, this cone complement has a hole in the middle to obtain a sort of funnel. We then made a vertical sawcut through half of the cone complement, after this, a coil made of *NbTi* wire is wrapped around it (see figure 3.3).

The coil around the cone complement will induce a magnetic field inside of it. But since the cone complement is made of Niobium which is superconducting under 10K, a Meissner-effect induced current starts to flow in the opposite direction to counteract this magnetic field. And since current in superconductors only flow along the outside of the material, the current will run as shown in figure 3.4. Thanks to the design of this cone complement, all of the current will flow through a very small part around the middle hole. This current is $\frac{N_p}{N_s} = 70$ times larger than the current running through the coil around the cone complement. For this coil we calculate from equation 2.6 that $L = 6.9\mu H$.

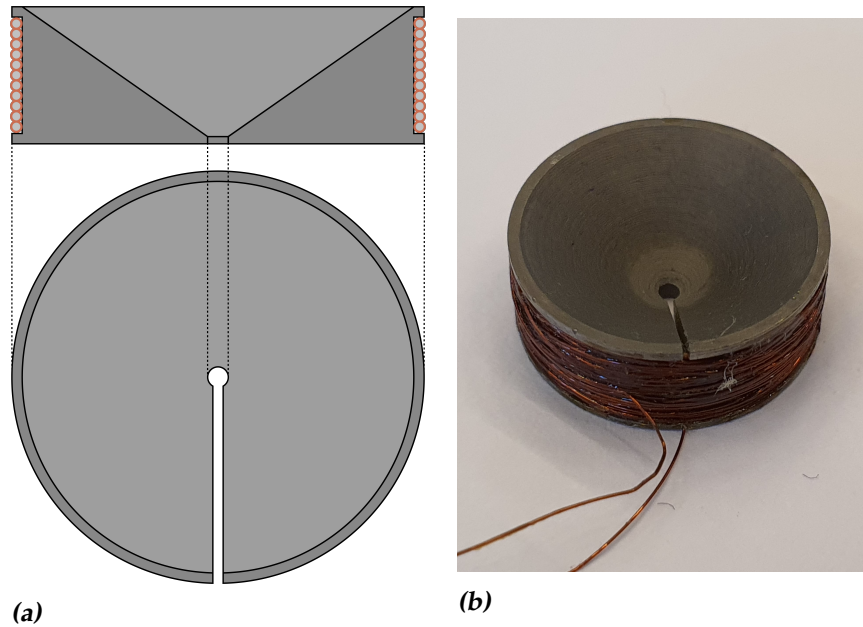


Figure 3.3: a) A sketch of the Cone Complement. Upper picture is a cross section as looked from the side with the wires of the coil around it, lower is the top view on which the sawcut can be seen. b) A photo of the cone complement coil.

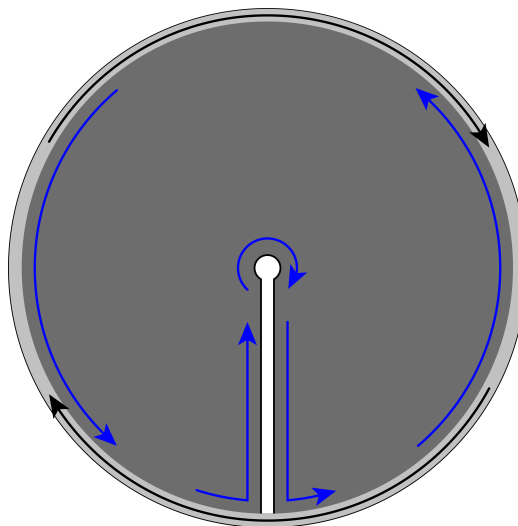


Figure 3.4: The current inside the cone complement.

4

Results

Here, the results of our measurements are presented in the same order as they are described in chapter 3, *Methodology*.

4.1 High Currents

For the high current measurements, multiple designs were considered. The first heatsink measurements were done at 3K with a normal loop without a heatsink (like in figure 4.2b) and a loop connected to a spotwelded heatsink (figure 3.1), the results are shown in figure 4.1.

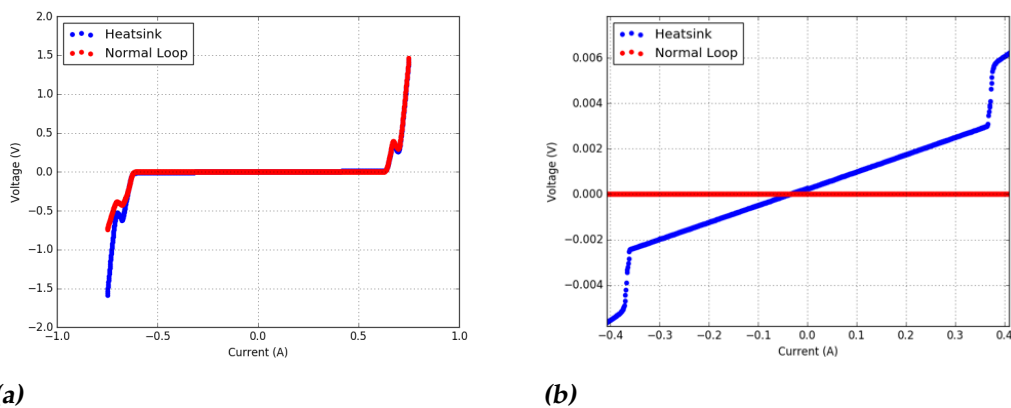


Figure 4.1: The heatsink versus the normal loop at the 3K plate. Figure a) shows the complete measurement from $-0.75A$ to $0.75A$. In b), a zoomed in version better shows the starting resistance in the heatsink.

In the next cooldown, the high current experiments were done on the mixing chamber plate at about $20mK$. First we have a normal shortcut loop in which the NbTi wire is directly soldered into the contact with normal solder. The results are shown below (figure 4.2).

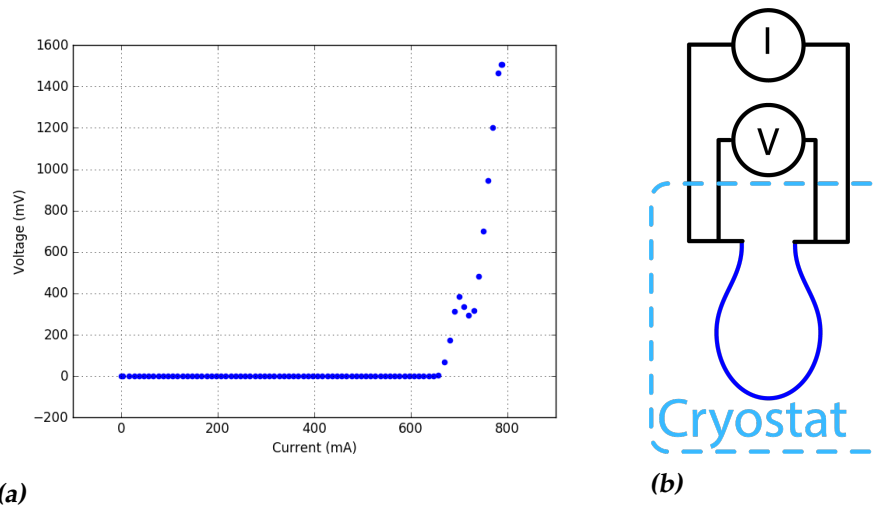


Figure 4.2: a) Shows the $V(I)$ measurement of the circuit shown in b), the dark blue line depicts the NbTi wire.

Figure 4.3 shows the results for the soldered heatsink explained in *Methodology*.

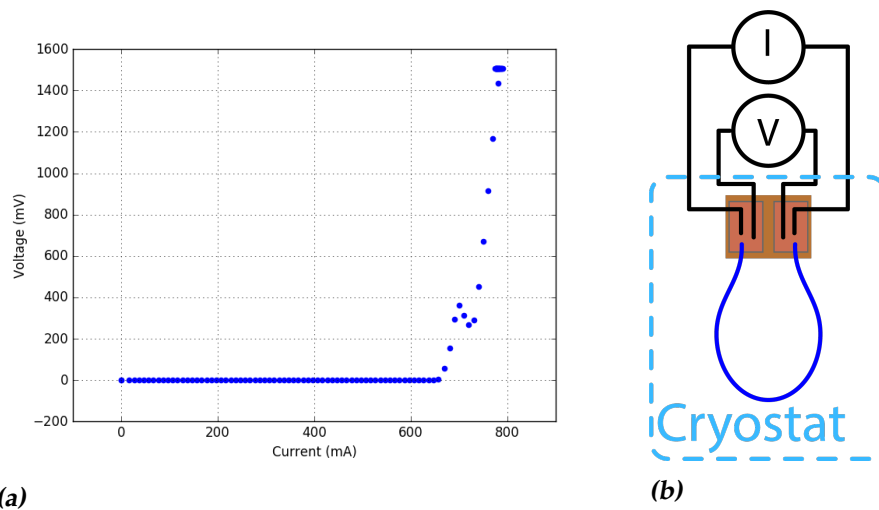


Figure 4.3: a) Shows the $V(I)$ measurement of the soldered heatsink of which the circuit is shown in b), the dark blue line depicts the NbTi wire.

Then, in figure 4.4, the results of the current splitter which was designed to distribute the current over multiple wires for a lower resistance per wire are shown.

In figure 4.5, the $V(I)$ plots of figures 4.2a, 4.3a and 4.4a are combined

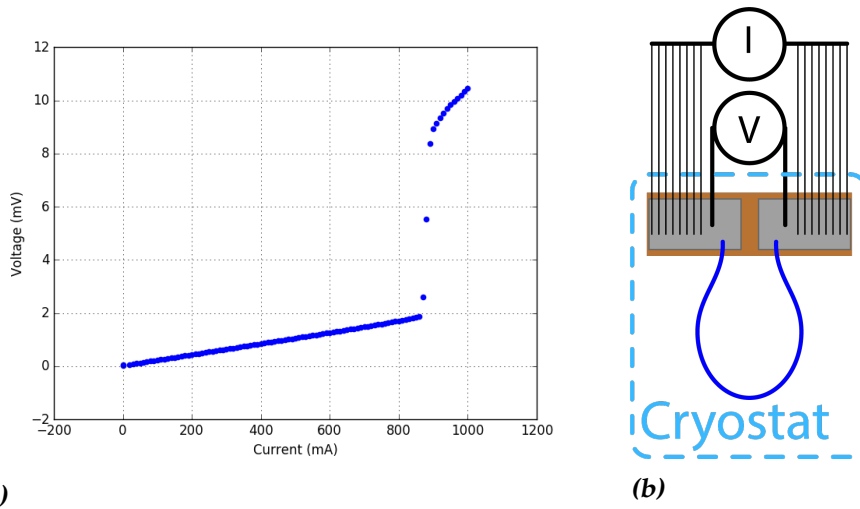


Figure 4.4: a) Shows the $V(I)$ measurement of the current splitter of which the circuit is shown in b), the dark blue line depicts the NbTi wire.

into one figure to better compare them. Figure 4.6 shows the dissipated power of these methods as a function of the current.

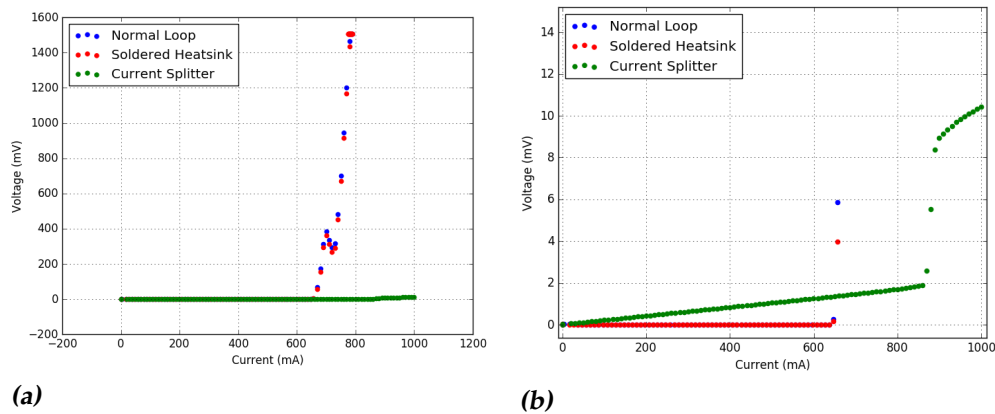


Figure 4.5: In a) the $V(I)$ curves of the normal loop, the soldered heatsink and the current splitter are shown in one figure. b) Shows the zoomed in version of this figure.

Lastly, a version of the spotwelded heatsink experiment with Niobium sheets with a larger area compared to the measurement in the *Marshmallow* was done in the *Yeti* at 5K. The results are shown in figure 4.7.

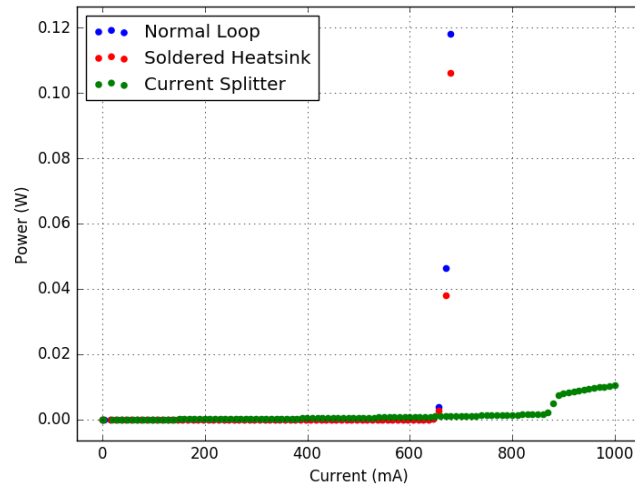


Figure 4.6: The dissipated power as a function of the current for the normal loop, the soldered heatsink and the current splitter.

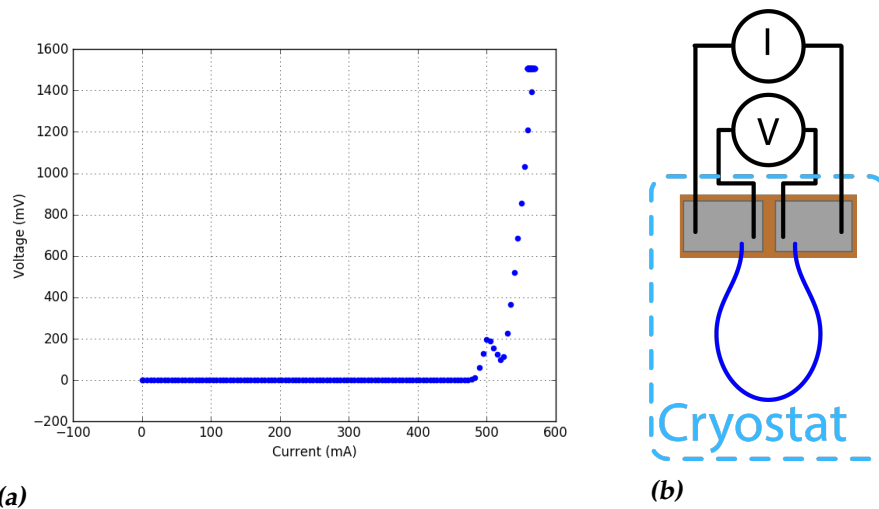


Figure 4.7: a) Shows the $V(I)$ measurement of the spotwelded heatsink in the Yeti of which the circuit is shown in b), the dark blue line depicts the NbTi wire.

4.2 Persistent Current Switch

To obtain a value for the inductance of the coil, a frequency sweep over the coil is conducted. The results are shown in figure 4.8. For every point of this figure, equation 2.7 can be filled in. The mean over these values

(while ignoring the first 3 points) yields for the inductance $L = 6.8\mu H^*$.

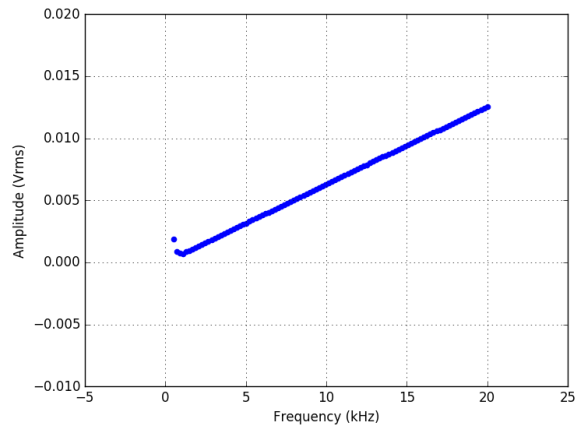


Figure 4.8: The voltage over the cone complement coil as a function of the frequency.

*Our input voltage failed to record, but based on an earlier measurement we calculated that our input voltage had to be around $500mV$. Inside the margins we set, the inductance ranges between $4\mu H$ and $7\mu H$

5

Discussion

5.1 High Currents

The results of the measurements with spotwelds show a starting resistance of $\sim 2m\Omega$ for the current splitter (figure 4.4a) at $20mK$, $\sim 2m\Omega$ for the spotwelded heatsink in the *Yeti* at $5K$ (figure 4.7a) and $\sim 7.5m\Omega$ for the spotwelded heatsink (figure 4.1) tested at $3K$. The difference in resistance of the heatsink at $3K$ can be explained by the quality of the spotweld. Since these are the only experiments with spotwelds and this starting resistance is not apparent in the other tests, we suspect this starting resistance to come from the spotwelds. This would, however, contradict with the $3p\Omega$ resistance B. van Waarde, O. Benningshof and T.H. Oosterkamp found for the resistance of a spotweld[5], so further research is needed. A proposal for an experiment is sketched in figure 5.1. A normal loop just like the loop in figure 4.2b is cut in half and the cut is then reconnected by spotwelding the two halves onto a sheet of *Nb* film. Furthermore, by placing multiple of these reconnected cables with spotwelds in series, the resistance should be shown to add up.

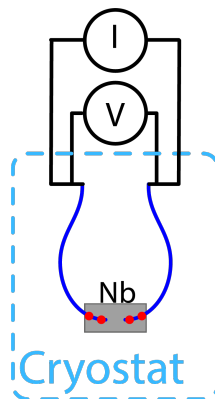


Figure 5.1: An experiment to find the resistance of a spotwelded contact, the spotwelds are depicted by the red dots.

5.2 Persistent Current Switch

Our results show our coil has an inductance of $6.8\mu H$, which is close to the calculated inductance in section 2.4. This inductance is low enough to be connected to the secondary side of a transformer without yielding too much backaction. This makes the following experiment sketched in figure 5.2 feasible.

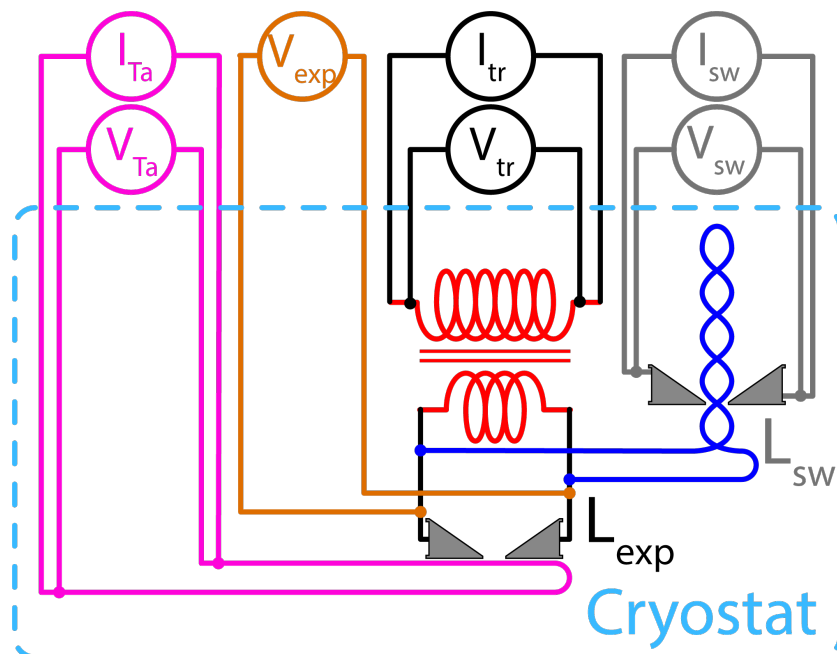


Figure 5.2: The circuit of the proposed experiment.

The idea of this experiment is to generate a B_0 field of $500mT$ in a Cone Complement coil which is here called L_{exp} . This coil is connected to a persistent current switch with a *Tantalum* ($H_C = 0.09T$ [10]) shortcut wire (blue line and grey circuit) to obtain a low noise signal. The coil of this persistent current switch (L_{sw}) is also made of a Cone Complement coil. To obtain a higher field in the experiment coil, it is placed on the secondary side of a Metglas transformer[11](red part in figure 5.2) with $N_p = 1000$ and $N_s = 1$. This makes it possible to obtain an I_s of about $5A$ to $10A$ while only sending currents of around $5mA$ to $10mA$ through the resistive parts of our circuits. This way, the heating inside the cryostat is minimized. Last, another wire made of *Tantalum* (pink circuit) is run close to the experiment coil. The moment the field at the center of the experiment coil is $500mT$, it should be $96mT$ at a distance of $1.8mm$. So the moment the tantalum wire at $1.8mm$ from the center of the coil changes its state from superconducting to normal, a field of $500mT$ is achieved in the center of the cone complement.

5.3 B_1 possibilities

It is also possible to use the cone complement for the B_1 field. To further investigate this, the coupling between the coil and the cone complement must be investigated. Two copies of the cone complement are already constructed, one made of copper and one made of Polyether ether ketone (PEEK). Around them a coil ($630\mu m$ isolated copper) with 8 windings is constructed while keeping them as similar as possible. From the measured difference in inductance between the two versions the coupling between the copper cone complement and the coil around it can be calculated since PEEK does not conduct electricity. By the same calculation as in section 2.4, we would obtain a coil of about $35.5nH^*$. For this coil to excite protons at about $50mT$, a resonance frequency of $\sim 2MHz$ is needed. Via

$$f_{res} = \frac{1}{2\pi\sqrt{LC}} \quad , \quad (5.1)$$

we find that to get an LC circuit with $f_{res} = 2MHz$ a capacitor of $178nF$ is needed. For the cone complement coil of $6.9\mu H$, a capacitor of $918pF$ has to be used.

*With $N_p = 8$, $\tilde{N}_p = 6$ and the other parameters staying the same.

6

Conclusion

We have discussed and tested various methods to send higher currents at milliKelvin temperatures to lower the dissipation over the resistive elements inside our dilution refrigerator. We have shown that a heatsink does not make a discernable difference for the critical current that can be sent through a wire inside the dilution refrigerator. Our results show that it is possible to send $0.6A$ without heating the mixing chamber. We have also shown that a soldered contact is less resistive than a spotwelded contact. Furthermore, we have devised and began testing a method for generating high B_0 -fields free of typical source noise and strong MHz B_1 -fields for use in extremely low temperature MRFM.

6.1 Acknowledgments

I have had a great time during this master research. First, I want to thank Tjerk for giving me the opportunity to do this research. He was always available for a small talk and is an interesting person to talk to. Most of my days were spend with Tim, thanks for being such a nice and helpful person. You were always available for questions and even though you made me feel really stupid some times, I have learned a lot from you. I will miss the daily joking around and trying to trigger you to get mad at Ruben and me by making up stupid "physics life hacks". Then Ruben, the other half of "Rummy", a name made up by Freek for us doing everything together in the first half of my research. Thanks for the daily discussions, helping to trigger Tim and for the walks to the station at the end of a research day. Without you, YouTube would not be as interesting as it is now with Melanie, Filip, Mrad, Stan, Jeppe and of course many more. Freek was always available to help and I also have learned a lot from you. Thanks for the interesting topics during lunch which sometimes had to be changed by Tjerk or Gesa for being too "graphic". Gesa helped a lot with

my understanding of the experiments and I want to thank you for the soccer games we played with the group. Thanks to Victor and Timothy for reminding me to go home on time to not be late for work, I really appreciated it. Furthermore, I want to thank Merlijn for constructing everything I needed for my experiments. I also want to thank Kier for helping with the design for the cone complement coil. Thanks to Jean-Paul for the fruitful conversations and supplying me with a breakfast the early mornings I did not have time to make breakfast at home.

Outside of school, I would like to thank my colleagues at Hoogvliet 660. After long days in the lab, they worked hard and were always in for fun conversations.

Bibliography

- [1] A. Vinante, M. Bahrami, A. Bassi, O. Usenko, G. Wijts, and T.H. Oosterkamp. Upper bounds on spontaneous wave-function collapse models using millikelvin-cooled nanocantilevers. *Physical Review Letters*, 116(9):090402, 2016.
- [2] Nadine Barrie Smith and Andrew Webb. *Introduction to Medical Imaging*. Cambridge University Press, 2011.
- [3] J. A. Sidles. Noninductive detection of single-proton magnetic resonance. *Applied Physics Letters*, 58(24):2854–2856, 1991.
- [4] M. de Wit, G. Welker, J.M. de Voogd, and T.H. Oosterkamp. Density and T_1 of surface and bulk spins in diamond in high magnetic field gradients. *Physical Review Applied*, 10(6):064045, 2018.
- [5] Bob van Waarde, Olaf Benningshof, and Tjerk Oosterkamp. A magnetic persistent current switch at milliKelvin temperatures. *Cryogenics*, 78, 2016.
- [6] A. T. A. M. de Waele. Basic operation of cryocoolers and related thermal machines. *Journal of Low Temperature Physics*, 164(5):179–236, 2011.
- [7] P. Das, R. Bruyn de Ouboter, and K. W. Taconis. A realization of a london-clarke-mendoza type refrigerator. In J. G. Daunt, D. O. Edwards, F. J. Milford, and M. Yaqub, editors, *Low Temperature Physics LT9*, pages 1253–1255, Boston, MA, 1965. Springer US.
- [8] G. Frossati. OBTAINING ULTRALOW TEMPERATURES BY DILUTION OF ^3He INTO ^4He . *Le Journal de Physique Colloques*, 39:C6–1578–C6–1589, 1978.
- [9] M. Lubell. Empirical scaling formulas for critical current and critical field for commercial nbt. *IEEE Transactions on Magnetics*, 19(3):754–757, May 1983.
- [10] R. W. Shaw, D. E. Mapother, and D. C. Hopkins. Critical fields of superconducting tin, indium, and tantalum. *Phys. Rev.*, 120:88–91, Oct 1960.

- [11] Freek Hoekstra. Fridge Magnets. Master's thesis, Leiden University, December 2018.